Preprint (submitted version, November 2026). Manuscript under peer review. No new archaeological site is confirmed. Open anonymized dataset and verification scripts: https://doi.org/10.5281/zenodo.24511141 (CC BY 4.0).

Auditing LiDAR terrain-anomaly candidates in Slovenia: spatial-block validation and reversible confounder narrowing

Daniele Corso · Independent researcher, Trieste, Italy
ORCID: 0009-0001-1691-1912 · Correspondence: corso.danie@gmail.com

Abstract

Airborne laser scanning reveals sub-canopy microtopography across karstic and forested terrain, but automated anomaly detectors produce large candidate sets heavily affected by natural landforms and recent land use. This paper audits a frozen cohort of 200 ranked hilltop terrain anomalies derived from the 2023-2025 Slovenian national LiDAR campaign (CLSS) and evaluates the parent regional pool of 186,606 labeled proposals across 210 ten-kilometre spatial blocks. In out-of-fold tests against registry-matched hillforts (n = 715; base rate 0.383%), a multi-feature ensemble ranker (Average Precision [AP] = 0.1152, 95% block-bootstrap CI [0.0804, 0.1504]; ROC-AUC = 0.9048 [0.8892, 0.9185]; Precision@200 = 0.310 [0.210, 0.400]) outperforms single-feature topographic dominance (AP = 0.0142 [0.0115, 0.0177]) by 8.12-fold. Stratified by detector morphology, hilltop-enclosure proposals (AP = 0.2425 [0.1646, 0.3197]; Recall@200 = 0.3198) outperform radial-ridge proposals (AP = 0.0669 [0.0483, 0.0957]; Recall@200 = 0.0760) by 3.63-fold in AP. Cross-referencing the 200 anomalies with official heritage registers (RNPD, ISKD_RNPD_OP), archaeological catalogues (Arkas, Zbiva), published LiDAR vectors, 1:100,000 geology (OGK100), point-cloud ground support (GKOT), and multi-period orthophotos retains 187 active unverified candidates, of which 96 (51.3%) show explicit modern or contextual confounders. Deterministic screening narrows the active list to a 38-candidate Tier 1 shortlist, including 16 hilltop-enclosure convergent records and 5 ground-supported clean records (3 meeting both criteria: L8, L34, L49). No new archaeological site is confirmed. The workflow provides an auditable triage step prior to specialist desk review and permitted non-invasive field checks.

Keywords: airborne LiDAR, archaeological prospection, Slovenia, Karst, spatial cross-validation, confounder audit, hillforts

1. Introduction

Airborne laser scanning (ALS) is widely used to document microtopographic remains beneath forest canopy on the Slovene and Italian Karst (Kras) (Bernardini, 2023; Lozić & Štular, 2021, 2024; Štular et al., 2021). Even with high-resolution digital terrain models (DTMs), remote morphological detection faces equifinality. Circular banks, hilltop

enclosures, and linear ridges can represent prehistoric or historic earthworks, but they also arise from post-medieval agricultural terraces, forestry tracks, quarrying, modern infrastructure, or natural carbonate outcrops.

Recent methodological studies keep four stages separate: automated anomaly detection, comparison with heritage registers and published inventories, verification of point-cloud ground support, and independent archaeological interpretation and dating (Lozić & Štular, 2021, 2024; Štular et al., 2021). At regional scale, two practical problems recur. Random patch splits can inflate accuracy estimates because nearby terrain patches share local geomorphology and survey properties. In addition, the top of a ranked candidate list often still holds too many modern or natural confounders for efficient specialist review.

Following the release of the 2023-2025 Slovenian national LiDAR campaign (CLSS) at 0.5 m DTM spacing by the Surveying and Mapping Authority of the Republic of Slovenia (GURS, 2026), this study examines a frozen regional candidate dataset to answer two questions. Under 10 km spatial-block out-of-fold validation across 186,606 proposals, how much does a multi-feature ranker improve on single-feature topographic baselines, and how does precision vary by morphological generator? Inside a frozen cohort of 200 top-ranked anomalies, what share of active proposals is affected by explicit modern or contextual confounders, and how far can deterministic, reversible screening reduce the specialist review queue without claiming unverified discoveries?

2. Materials and methods

2.1 Airborne LiDAR data and proposal generators

All spatial analyses used the Slovenian national projected coordinate reference system D96/TM (EPSG:3794). Terrain derivatives were computed from 1,828 sheets of the GURS CLSS 2023-2025 0.5 m digital terrain model (DMR, CC BY 4.0) covering the Kras region and adjoining areas of Slovenia (GURS, 2026). On 11 priority sheets, supplementary observational checks used 4.836 GB of classified point clouds (GKOT; 453,768,678 decoded points) and digital surface models (DMP). Tiles were processed with neighbourhood halos to prevent edge artifacts in local relief and openness filters (Lozić & Štular, 2021; Štular et al., 2021).

Two morphological generators produced the parent regional pool (N = 195,369 total proposals; 186,606 labeled after excluding 8,763 ambiguous buffer rows). The A2 generator (`A2v02`) detects positive-relief enclosures using a 10 m simple local relief model (SLRM) radius, a 0.30 m minimum bank height, 3 m morphological gap closing, and area limits of 600 to 120,000 m². Its outputs are split into `A2v02_hilltop_enclosure` (N = 46,764), `A2v02_depression_enclosure` (N = 21,504), and `A2v02_flat_enclosure` (N = 13,498). The A3 generator (`A3pool`, N = 104,840) starts from candidate summits and tests radial ridge organization across radii from 15 m to 150 m in 2.5 m steps and 36 angular sectors.

An ensemble ranker (Ranker v1.2: 15 ExtraTrees classifiers, 150 trees per member, minimum 3 samples per leaf, square-root feature selection, and up to 10:1 negative subsampling) was evaluated out-of-fold with 10-fold spatial-block cross-validation over 10 km × 10 km blocks (`seed = 20261103`). Positive labels (n = 715) correspond to proposals within 50 m of a registered hillfort point; background negatives (n = 185,891) lie more than 300 m from any registered archaeological entry. Because unrecorded sites can exist in the background class and positive labels target hillforts specifically, ranker scores are operational priority indices and are not calibrated probabilities of archaeological truth.

2.2 Spatial-block statistical evaluation

Out-of-fold predictions across the 186,606 labeled proposals (210 ten-kilometre blocks) were scored with Average Precision (AP), ROC-AUC, Precision@K, Recall@K, and Lift@K (K = 100, 200, 500, 1000, 2000). Ranker v1.2 was compared against two non-learned morphological baselines (`dominance_250m` and `ring_radius_m`) and stratified by generator source. To account for spatial clustering within landscape blocks, 95% confidence intervals were estimated with 200-replicate cluster bootstrap resampling over the 210 spatial blocks (`seed = 20261124`).

2.3 Documentary, geological, and observational cross-checks

A frozen cohort of 200 top-ranked locations (L1-L200; 140 from `A3pool` , 60 from `A2v02_hilltop_enclosure`) was cross-referenced in EPSG:3794 against five groups of institutional and published sources. Official heritage checks used 31,107 representative points from the Slovenian Register of Immovable Cultural Heritage (RNPD, OPSI CC BY 4.0 export; Ministrstvo za kulturo, 2026a) and 10 native polygons retrieved via ID-first queries within 150 m from `ISKD_RNPD_OP` (Layer 3312; Ministrstvo za kulturo, 2026b). Both legacy `MK_EVRD` and `MK_ARHEO` endpoints returned HTTP 404 (`Service not found`), so prior archaeological-investigation coverage is recorded as unknown.

Archaeological literature checks used the Arkas 2.0 public GIS (`Arkas20_Apr23` , 93 unique points within 1 km; ZRC SAZU, 2026), Zbiva v4.1 (3,914 records, 3,828 geolocated; Belak et al., 2023), and published LiDAR interpretation vectors for Kostanjevica and Lipe (393 lines and 369 points transformed from EPSG:3912 to EPSG:3794; Lozić & Štular, 2022). Geological context came from the GeoZS Basic Geological Map 1:100,000 (OGK100; GeoZS, 2026), which covers all 200 centres across 136 geological units. Nine source polygons contained ring self-intersections and were repaired in derived analytical copies using GEOS `make_valid` (12 affected candidates flagged; raw geometries untouched). Lithologies were grouped into four coarse context classes (`carbonate_karst` , `flysch_siliciclastic` , `other_bedrock` , `quaternary_unconsolidated`), noting that bedrock age does not date surface features.

Observational ground support was measured from GKOT point clouds in 2 m cells after excluding withheld and overlap points. Ring samples within 4 m of an occupied ground cell were counted as supported, requiring at least 75% ring support for `GROUND_SUPPORTED` . Multi-period GURS DOF025 orthophoto mosaics (2017-2019 and 2022-2024; GURS, 2026) were screened for contemporary buildings, roads, cultivation, quarries, and earthmoving.

2.4 Reversible queue screening and deterministic narrowing

First-stage audit screening retained 187 active unverified proposals and moved 13 cases to separate audit dispositions without changing original scores or coordinates: 7 mapped-context exclusions (L41, L54, L110, L118, L145, L175, L186), 2 likely contemporary structures (L116, L138), 1 geometric duplicate at disk IoU >= 0.40 (L77 overlapping L23, IoU = 0.4957), and 3 holds where an Arkas point falls inside the proposal disk (L92, L109, L182).

Second-stage deterministic narrowing assigns each active candidate to one of seven mutually exclusive, reversible tiers. Tier T4 (`DEPRIORITIZED_HIGH_CONFOUNDER`) collects active quarry or earthmoving cases (`TRASFORMAZIONE_RECENTE`) and non-transitive secondary disk overlaps at IoU >= 0.25. Tier T3 (`CONFOUNDED_LAND_USE_OR_CONTEXT`) collects proposals with mapped buildings inside the ring (`buildings_in_ring > 0`), visible modern cultivation, roads, or adjacent ruins (`GESTIONE_VISIBILE` , L6, L18), partial `ISKD_RNPD_OP` edge overlap, or an Arkas reference within 300 m. Tier T2 (`UNCONFOUNDED_NEEDS_LIDAR_OR_BUILDING_QC`) holds proposals with unconfounded orthophoto cover (`BOSCO_ROCCIA` or `RADURA_INDETERMINATA`) that lack a retained original LiDAR crop, lack a building count, or sit on unconsolidated

Quaternary deposits. Tier T1 (`PRIMARY_SHORTLIST`) requires zero mapped buildings in the ring, unconfounded land cover, bedrock substrate, no T3 or T4 flags, and a retained original LiDAR crop. It splits into T1A-A2 (GKOT ground-supported with A2 hilltop support), T1A-A3 (GKOT ground-supported, A3-only), T1B-A2 (unassessed GKOT with A2 hilltop support), and T1B-A3 (unassessed GKOT, A3-only).

3. Results

3.1 Spatial-block discrimination and generator stratification

Table 1 and Figure 1 report out-of-fold discrimination across the 186,606 labeled regional proposals (715 registry hillfort positives across 210 ten-kilometre blocks).

Table 1. Out-of-fold spatial-block discrimination across 186,606 regional LiDAR proposals with 200-replicate 10 km block-bootstrap 95% confidence intervals.

Model / generator stratum	N	Positives	AP [95% block CI]	ROC-AUC [95% block CI]	P@200 [95% CI]	R@200 [95% CI]	Lift@200
Ranker v1.2 (OOF, all sources)	186,606	715	0.1152 [0.0804, 0.1504]	0.9048 [0.8892, 0.9185]	0.310 [0.210, 0.400]	0.0867 [0.0613, 0.1074]	80.9×
Baseline: `dominance_250m`	186,606	715	0.0142 [0.0115, 0.0177]	0.8390 [0.8160, 0.8583]	0.000 [0.000, 0.000]	0.0000 [0.0000, 0.0000]	0.0×
Baseline: `ring_radius_m`	186,606	715	0.0065	0.6119	0.035	0.0098	9.1×
`A2v02_hilltop_enclosure`	46,764	197	0.2425 [0.1646, 0.3197]	0.9425 [0.9276, 0.9578]	0.315 [0.220, 0.420]	0.3198 [0.2539, 0.3804]	74.8×
`A3pool`	104,840	513	0.0669 [0.0483, 0.0957]	0.8590 [0.8348, 0.8820]	0.195 [0.130, 0.255]	0.0760 [0.0515, 0.0957]	39.9×
`A2v02_flat_enclosure`	13,498	3	0.0024	0.8827	0.000	0.0000	0.0×
`A2v02_depression_enclosure`	21,504	2	0.0012	0.9424	0.000	0.0000	0.0×

Ranker v1.2 outperforms `dominance_250m` by 8.12-fold in AP (reaching Precision@100 = 0.450, 117.4× lift, and Precision@200 = 0.310, 80.9× lift), with non-overlapping 95% block-bootstrap confidence intervals. Across generators, `A2v02_hilltop_enclosure` beats `A3pool` by 3.63-fold in AP and 4.21-fold in Recall@200, again with disjoint 95%

confidence intervals. Flat enclosures (3 positives in 13,498 proposals) and depression enclosures (2 positives in 21,504 proposals) carry almost no hillfort signal.

3.2 Confounder audit and active-queue narrowing

No geolocated Zbiva entry and no published Kostanjevica/Lipe vector lies within 300 m of the 200 proposals. Twenty-one proposals have an RNPD representative point within 300 m (none inside a disk). Three active proposals show small (<3% area) `ISKD_RNPD_OP` edge overlaps (L19, L52, L87) without centre containment, and three have an Arkas reference within 300 m (L9, L80, L81). Among the 187 active candidates, GKOT ground support is complete for 11, partial for 3, and unassessed for 173; retained original LiDAR crops exist for 96 and are flagged as missing for 91. On OGK100, 132 active centres fall on carbonate karst, 44 on flysch or siliciclastic units, 6 on other bedrock, and 5 on unconsolidated Quaternary sediments (Figure 3).

Table 2 and Figure 2 show the resulting stratification of the 187 active candidates and the distribution of explicit confounders.

Table 2. Deterministic stratification of the 187 active unverified candidates.

Narrowing tier	Count	Share of 187	Operational role and defining criteria
`T1A_CORE_GROUND_SUPPORTED_A2`	3	1.6%	Priority core: GKOT ground-supported, A2 hilltop support, 0 buildings, clean cover, bedrock, LiDAR crop (L8, L34, L49)
`T1A_CORE_GROUND_SUPPORTED_A3`	2	1.1%	GKOT ground-supported clean core, A3-only morphology (L26, L62)
`T1B_CLEAN_LIDAR_A2_CONVERGENT`	13	7.0%	Unassessed GKOT, clean cover, 0 buildings, bedrock, LiDAR crop, A2 hilltop support (L11, L12, L15, L20, L22, L53, L58, L63, L68, L69, L83, L84, L96)
`T1B_CLEAN_LIDAR_A3_ONLY`	20	10.7%	Unassessed GKOT, clean cover, 0 buildings, bedrock, LiDAR crop, A3-only
`T2_UNCONFOUNDED_NEEDS_LIDAR_OR_BUILDING_QC`	53	28.3%	Clean orthophoto cover but missing retained LiDAR crop, missing building count, or Quaternary substrate
`T3_CONFOUNDED_LAND_USE_OR_CONTEXT`	93	49.7%	Mapped buildings in ring (29), visible modern cultivation, roads, or adjacent ruin (88), ISKD edge overlap (3), or Arkas < 300 m (3)
`T4_DEPRIORITIZED_HIGH_CONFOUNDER`	3	1.6%	Active quarry or earthmoving (L66, L195) or secondary overlap at IoU >= 0.25 (L80 vs L9, IoU = 0.345)

In total, 96 of 187 active candidates (51.3%) carry explicit modern structural, land-use, overlap, or nearby-inventory confounders (T3 and T4). The reversible triage funnel narrows the workload from 200 frozen anomalies to 187 active

proposals, then to 38 Tier 1 low-confounder candidates, 16 A2-convergent clean records, and 5 GKOT ground-supported clean records (3 combining GKOT support and A2 convergence: L8, L34, L49). Threshold sensitivity checks show 2 suppressed overlap pairs at IoU >= 0.25 (L77/L23 and L80/L9), 1 at IoU >= 0.40 (L77/L23), and 0 at IoU >= 0.50. Proximity buffers of 100, 300, and 500 m match 3, 21, and 61 candidates in RNPD, and 3, 6, and 14 in Arkas.

4. Discussion

The spatial-block results show that multi-feature ranking improves substantially over single-feature topographic dominance (8.12-fold in AP), but detector morphology remains decisive. Proposals from `A2v02_hilltop_enclosure` achieve 3.63-fold higher AP and 4.21-fold higher Recall@200 than `A3pool`, while flat and depression enclosures contribute almost pure background noise for hilltop-fortification targets. Prioritizing candidates supported by A2 hilltop containment therefore rests directly on measured regional performance.

The confounder audit also explains why automated LiDAR rankings cannot be read as site inventories. Even within the top 200 ranked anomalies across Slovenia, 51.3% of active proposals involve mapped buildings inside the ring, visible modern agriculture or roads, active quarrying or earthmoving, or adjacent registered heritage. Comparing administrative and research sources proved necessary: three candidates without an RNPD point inside their disk contained an Arkas published-site point, because administrative registries and research catalogues differ in thematic scope and update schedules.

Explicit reporting of missing evidence matters as much as documenting positive matches. Because `MK_ARHEO` was unavailable (HTTP 404), 86 Zbiva entries lack coordinates, and 173 active candidates lack full GKOT assessment, absence from checked inventories cannot prove novelty. Narrowing the active list to 38 Tier 1 candidates (led by the 5 GKOT ground-supported clean cases L8, L26, L34, L49, L62 and 13 A2-convergent cases prioritized for GKOT retrieval) makes blind specialist desk review and subsequent permissioned non-invasive field visits realistic. To avoid unpermitted ground disturbance under Slovenian heritage legislation, exact coordinates are omitted from public release and generalized to 5 km × 5 km EPSG:3794 grid cells, while full-precision dossiers remain restricted to competent heritage authorities and accredited researchers.

5. Conclusion

Pairing 10 km spatial-block bootstrap validation over 186,606 regional LiDAR proposals with a reversible multi-source confounder audit quantifies both the discriminatory strength of hilltop-enclosure detectors (3.63× AP over radial-ridge proposals; 8.12× AP over topographic dominance) and the prevalence of modern or contextual confounders (51.3%) among top-ranked anomalies. Deterministic screening narrows 187 active unverified candidates to a 38-candidate Tier 1 shortlist (5 GKOT ground-supported clean core records, 3 with A2 convergence: L8, L34, L49) suited for blind specialist review. No new archaeological site is claimed; independent archaeological assessment remains required before chronological attribution or predictive calibration.

Data and code availability

The open CC BY 4.0 dataset (200-candidate anonymized audit, 187-candidate narrowed catalogue, 38-candidate Tier 1 shortlist generalized to 5 km × 5 km EPSG:3794 grid cells, aggregate spatial-block validation metrics, source provenance and license register, and SHA-256 manifest) together with standalone MIT-licensed Python verification scripts and unit tests (4/4 passing, standard library only) is permanently archived on Zenodo at `https://doi.org/10.5281/zenodo.24511141` (Corso, 2026). Non-CC-BY raw third-party extracts are not redistributed. Exact EPSG:3794/WGS84 coordinates and full-resolution review dossiers are held privately to protect potentially vulnerable unverified locations and are available to competent heritage authorities and accredited researchers upon reasonable request to the author.

Acknowledgements

The author thanks the Surveying and Mapping Authority of the Republic of Slovenia (GURS), the Slovenian Ministry of Culture, the Geological Survey of Slovenia (GeoZS), and ZRC SAZU for maintaining public geospatial and heritage reference services. Cited researchers and institutions have not validated these candidate records and do not endorse the dataset.

Conflict of interest

The author declares no conflict of interest.

Figure captions

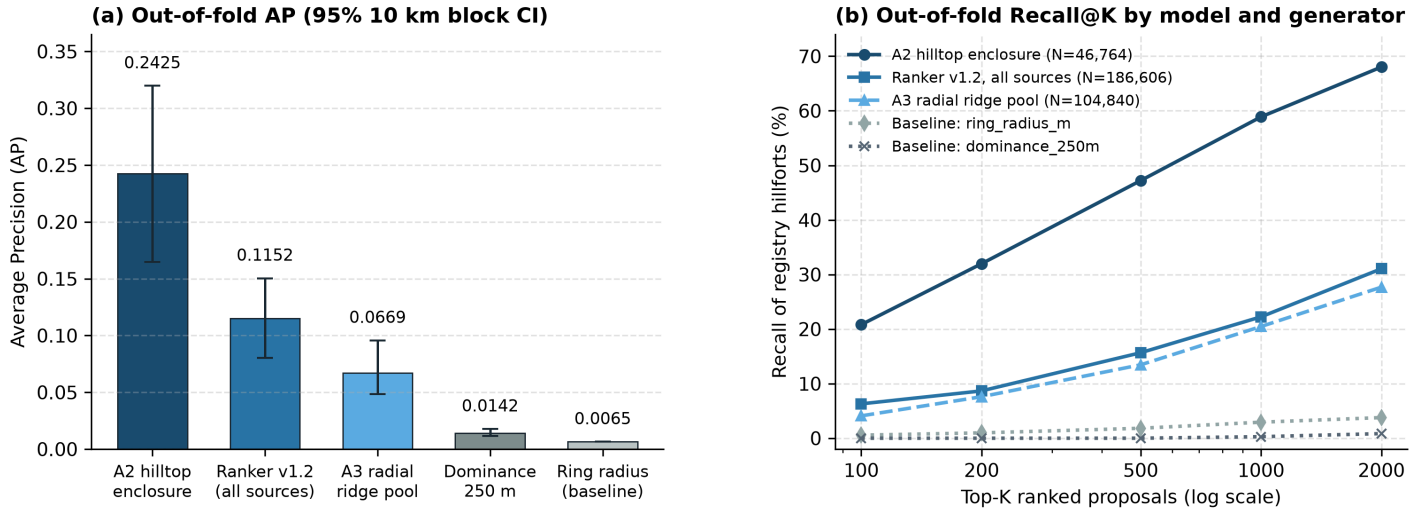


Figure 1. Out-of-fold spatial-block discrimination across 186,606 regional LiDAR proposals (210 ten-kilometre blocks, 715 registry hillfort positives). (a) Average Precision (AP) with 95% cluster-bootstrap confidence intervals comparing Ranker v1.2, generator strata (`A2v02_hilltop_enclosure` , `A3pool`), and single-feature morphological baselines (`dominance_250m` , `ring_radius_m`). (b) Out-of-fold Recall@K across K = 100 to 2,000 ranked proposals.

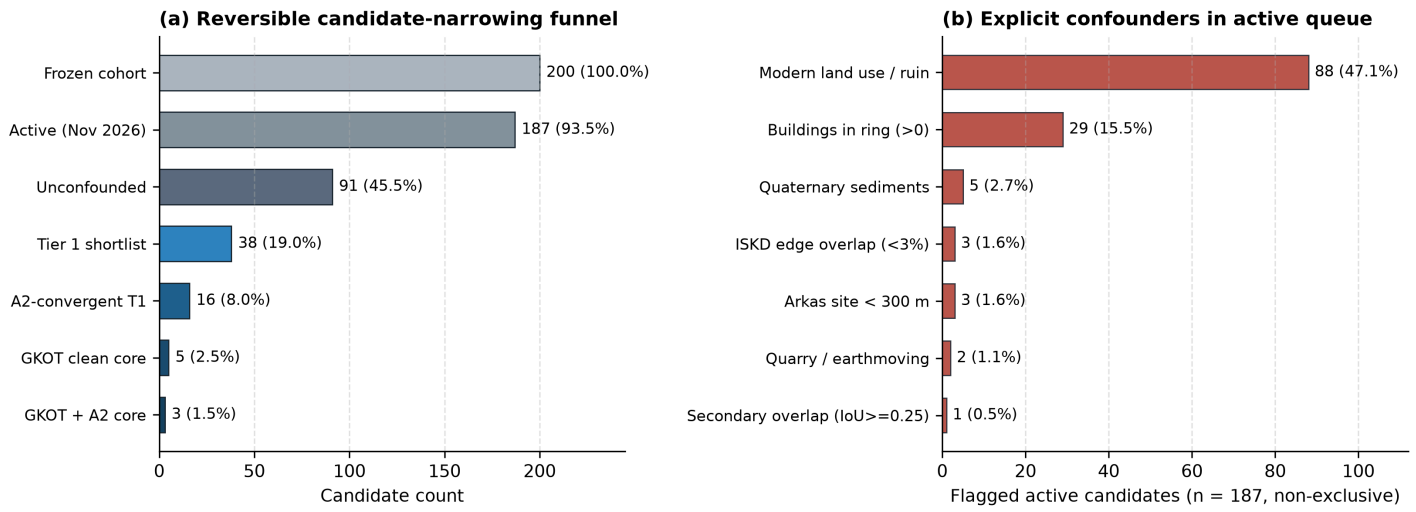


Figure 2. Reversible confounder audit and candidate narrowing. (a) Stepwise reduction from 200 frozen terrain anomalies to 187 active proposals, 91 unconfounded proposals, 38 Tier 1 low-confounder candidates, 16 A2-convergent Tier 1 candidates, 5 GKOT ground-supported clean core records, and 3 records combining GKOT support and A2 hilltop convergence (L8, L34, L49). (b) Frequency of explicit confounder flags among the 187 active candidates (flags are non-exclusive).

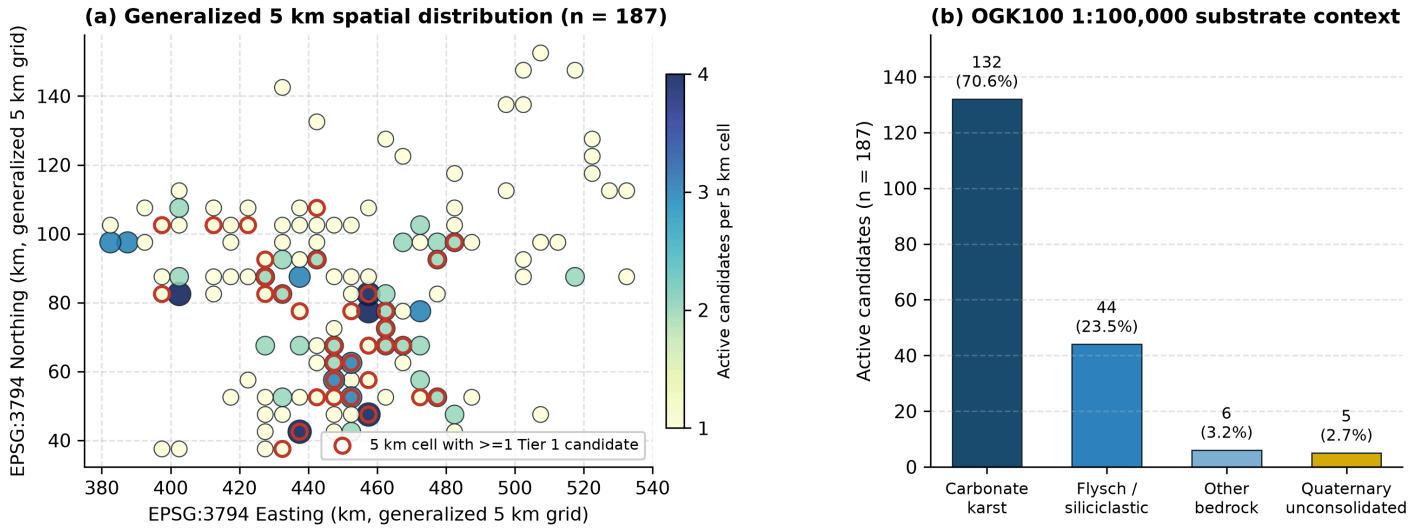


Figure 3. Generalized spatial and geological context of the 187 active candidates. (a) Spatial density aggregated to 5 km × 5 km EPSG:3794 grid cells (25 km^2; exact coordinates omitted), highlighting cells that contain at least one Tier 1 candidate. (b) Distribution of active candidate centres across coarse GeoZS OGK100 (1:100,000) lithological classes.

References

Belak, M., Pleterski, A., Rihter, J., & Štular, B. (2023). *Zbiva v4.1: Early medieval archaeological database*. ZRC SAZU. https://zbiva4.zrc-sazu.si/

Bernardini, F. (2023). Ancient roads and land divisions in the Trieste Karst revealed by airborne LiDAR. *Remote Sensing*, 15(6), 1506. https://doi.org/10.3390/rs15061506

Corso, D. (2026). *Audited LiDAR Terrain-Anomaly Candidate Dataset for Slovenia (Anonymized 5 km Grid, v5.0)* [Dataset]. Zenodo. https://doi.org/10.5281/zenodo.24511141

GeoZS (Geological Survey of Slovenia). (2026). *Basic Geological Map of Slovenia 1:100,000 (OGK100)*. https://gis.geo-zs.si/server/rest/services/OGK100/OGK100_feature/MapServer

GURS (Geodetska uprava Republike Slovenije). (2026). *CLSS 2023-2025 airborne LiDAR products (DMR, GKOT, DMP) and DOF025 orthophotos*. https://clss.si/ and https://www.e-prostor.gov.si/

Lozić, E., & Štular, B. (2021). Documentation of archaeology-specific workflow for airborne LiDAR data processing. *Geosciences*, 11(1), 26. https://doi.org/10.3390/geosciences11010026

Lozić, E., & Štular, B. (2022). *Archaeological LiDAR data, Kostanjevica na Krasu (Slovenia)* (Version 1.0) [Dataset]. Zenodo. https://doi.org/10.5281/zenodo.7357286

Lozić, E., & Štular, B. (2024). Archaeological LiDAR in Mediterranean karst landscapes: A multiproxy dating method and case study from the prehistoric Kras Plateau (Slovenia). *Archaeological Prospection*. https://doi.org/10.1002/arp.1954

Ministrstvo za kulturo Republike Slovenije. (2026a). *Register nepremične kulturne dediščine (RNPD)* [OPSI open-data export]. https://podatki.gov.si/dataset/register-nepremicne-kulturne-dediscine

Ministrstvo za kulturo Republike Slovenije. (2026b). *ISKD_RNPD_OP registered immovable heritage polygons (Layer 3312)*. https://geohub.gov.si/ags/rest/services/MK/ISKD/MapServer/3312

Štular, B., Lozić, E., & Eichert, S. (2021). Airborne LiDAR-derived digital elevation model for archaeology. *Remote Sensing*, 13(9), 1855. https://doi.org/10.3390/rs13091855

ZRC SAZU, Institute of Archaeology. (2026). *Arkas 2.0 archaeological cadastre and public GIS (Arkas20_Apr23)*. https://iza2.zrc-sazu.si/en/zbirka/arkas